A probabilistic theory for the strength of discontinuous fibre composites

FUMINORI HIKAMI*, TSU—WEI CHOU
Department of Mechanical and Aerospace Engineering, University of Delaware, Newark, Delaware 19711, USA

The strength of discontinuous fibre-reinforced composites is often reduced due to local stress concentrations at large fibre-end-gaps. A theoretical prediction of the strength of unidirectional fibre composites is performed based upon a probabilistic model of the fibre configuration. This work further develops the concepts of Bader, Chou and Quigley, and Fukuda and Chou. A limiting case of the present analysis shows good agreement with the results of Smith. Emphases are placed on the effect of matrix stress transfer properties including matrix plasticity. For a matrix deforming elastically, the strength is reduced as the composite size (N) increases. As compared with the rule-of-mixtures prediction for continuous fibre composites with identical fibre volume fraction, the reduction is shown to be proportional to $(\ln N)^{-P}$, with the exponent P being between 0.5 and 1 for two-dimensional composites and between 0.25 and 0.5 for three-dimensional composites. For a matrix deforming plastically, the local stress concentrations are reduced. Based upon the analytical expression of the local load sharing rule for a plastically deformed matrix, the composite strength is shown to approach the modified rule-of-mixtures of Kelly and Tyson as the matrix yield stress decreases.

1. Introduction

Discontinuous fibre reinforced metal and polymer composites are gaining increasing technological importance due to their versatility in properties and their high performance. Unlike continuous fibre composites the mechanical behaviour of discontinuous fibre composites is often dominated by the complex stress distributions due to fibre discontinuities [1–3]. In particular, the local stress concentration at fibre ends plays a critical role in affecting the performance of discontinuous fibre composites, and it often reduces the strength of a discontinuous fibre composite to a level far less than that of a continuous fibre composite with the same fibre volume content. Several theories [3] have been proposed to predict the strength of discontinuous fibre composites. One type of theory is based on the modification of the "rule-of-mixtures," which was originally developed for con-

tinuous fibre composites. Since the axial stress distribution in a discontinuous fibre is not uniform, the rule-of-mixtures has been modified by researchers to take into account the effect of fibre length.

Among discontinuous fibre composites, aligned fibre composites have many attractive properties for aeronautical application [4–6]. Kacir and Narkis [7] pointed out that when complicated shapes and double curvatures were to be fabricated by matched-die high-pressure moulding techniques, aligned discontinuous fibre composites had an advantage over their equivalent continuous mats. The ability of aligned fibre composite to elongate both parallel and perpendicular to the fibre direction without splitting, complements the predominant shear deformation of woven materials [5]. Because of their useful properties, highly aligned discontinuous fibre composites have been com-
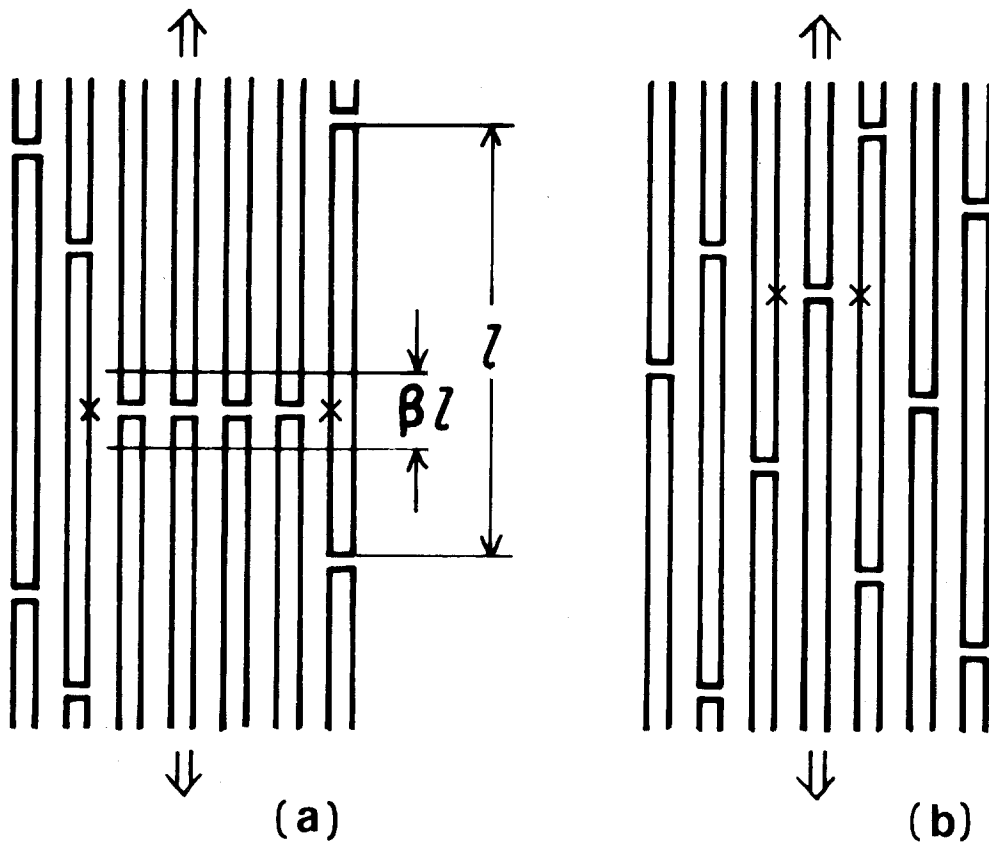
Figure 1 Schematic representation of fibre configuration. Sites of stress concentration are indicated by x.

mercially produced by the centrifuge [5] and vacuum [6] processes.

The present paper treats the case of aligned discontinuous fibre composites. The discontinuity of fibres gives rise to gaps between adjacent fibre ends. The collection of the adjacent fibre ends is termed a "fibre-end-gap" (see Fig. 1a). The width of a fibre-end-gap depends upon the number of fibre ends in the gap. The existence of a fibre-end-gap inevitably induces a stress concentration on the fibres bridging such a gap. Thus the fracture of a bridging fibre can take place at locations of high stress concentration while the stress level in most parts of the fibre is well below the ultimate strength. Such a failure mechanism needs to be taken into account in the modification of the rule-of-mixtures.

Bader *et al.* [8] first proposed the concept of a critical zone in dealing with short fibre composite strength and defined the fibres in the zone as either ending fibres or bridging fibres. Since the distribution of fibres is normally fairly random, it is essential to examine the strength of discontinuous fibre composites by a probabilistic method.

Fukuda and Chou [9] first adopted such an approach. In [9], the probability distribution of fibre-end-gap size was calculated using the concept of "critical zone". However, they did not consider the probability distribution of the maximum gap size which determines the strength of the composite.

A rigorous discussion on the probabilisitc aspect of the strength of discontinuous fibre composites has been given by Smith [10]. Using a two-dimensional chain-of-bundles model with the simplified assumption of local load sharing [10–16], Smith proved that no non-degenerate limit distribution [17] exists for the asymptotic strength of the system as the number of the fibres tends to infinity. This fact is quite contrary to the situation for the asymptotic strength of continuous fibre composites in which the existence of the limit distribution has been conjectured [12–15]. Smith also showed upper and lower bounds for the asymptotic strength of the system. The obtained bounds may be useful to inspect the validity of the physical models, although the simple assumption of local load sharing rule needs to be modified.
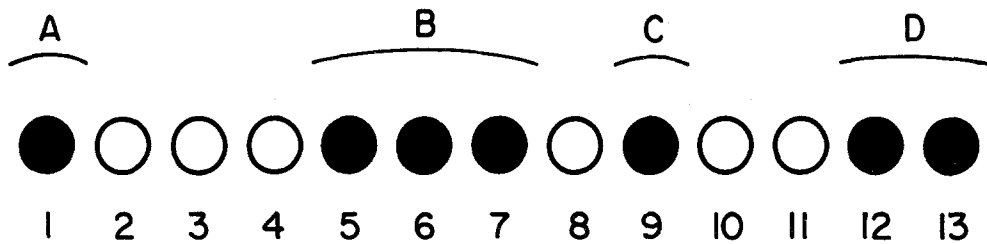
Figure 2 Schematic cross-sectional view of fibre configuration. Solid circles depict ending fibres and open circles indicate bridging fibres. A group of adjacent ending fibres is termed a fibre-end-gap (i.e., A, B, C and D).

In this paper a physical model is presented to examine the strength of unidirectional discontinuous fibre composites affected by local stress concentrations in two-dimensional and three-dimensional fibre arrays. The approximate probability distribution function for the maximum gap size is used to obtain the strength of composites. The matrix is assumed to deform elastically as well as elastically and perfectly-plastically. The local load sharing rule for the case of plastic matrix has been obtained by the authors [18] from the explicit solutions of a two-dimensional shear-lag analysis and it is incorporated into the probabilisitc approach. Since the matrix plastic deformation tends to disperse the local stress concentration, the strength of the composite is shown to approach the modified rule of mixtures obtained by Kelly and Tyson [19] as the matrix yield strength decreases.

2. Strength theory of two-dimensional fibre composites

It is assumed in the present analysis that the fibres are of uniform length and sufficiently long and failure of the composite occurs due to fibre breakage by local stress concentrations. Fig. 1 shows schematically the effect of fibre configuration on composite strength. Two typical examples of fibre configuration are considered. Case (a) obviously gives rise to comparatively larger stress concentrations on the bridging fibres at the locations marked by x than case (b). The stress at point x in case (a) reaches the fibre ultimate strength at the nominal composite strength level much lower than that of case (b). In the following we formulate the strength theory of discontinuous fibre composite affected by such large fibre-end-gaps.

2.1. Stress concentration factor
The composite is first modelled as a two-dimensional array of parallel discontinuous fibres of

length l. Following [8], the strength is examined for a critical zone of length βl with $0 < \beta \ll l$. The critical zone length is assumed to be of the same order of fibre ineffective length. In regard to the critical zone, a discontinuous fibre can end in the zone (ending fibre), in which case it bears no load, or it can bridge the zone (bridging fibre) and contribute to the strength of the critical zone. The probabilities of finding an ending fibre and a bridging fibre are β and $1 - \beta$, respectively. All fibres are assumed to have uniform strength σ_{fu}. Within each transverse section of the composite, ending fibres and bridging fibres are distributed randomly. A typical fibre configuration on a transverse section in a two-dimensional fibre array is shown in Fig. 2. The ending fibres and bridging fibres are depitcted, respectively, by solid circles and open circles. Under unit applied stress, the stress in the bridging fibres is enhanced by the stress transferred from the neighbouring ending fibres. For example, the stress in the bridging fibre No. 8 in this figure is enhanced by the ending fibres Nos. 1, 5, 6, 7, 9, 12 and 13. In other words, it is enhanced by the neighbouring fibre-end-gaps A, B, C and D.

Since stress concentration factor $(\bar{K})$ cannot be readily calculated by considering the enhancement effect from all the fibre-end-gaps, assumptions need to be introduced for the load sharing rule. The first and simplest lower value approximation for $\bar{K}$ is obtained by only considering the enhancement effects of the first nearest neighbouring fibre-end-gaps both from the right and left sides the bridging fibre. This assumption is allowable if the probability for finding the ending fibre is comparatively small. Then the stress concentration factor $\bar{K}_1^l$ can be calculated using the shear-lag method [20]. The second and third order lower value approximations ($\bar{K}_n^l$: $n = 2, 3$) are also obtained by taking into account the effects from the second and third nearest fibre-end-gaps, respec-
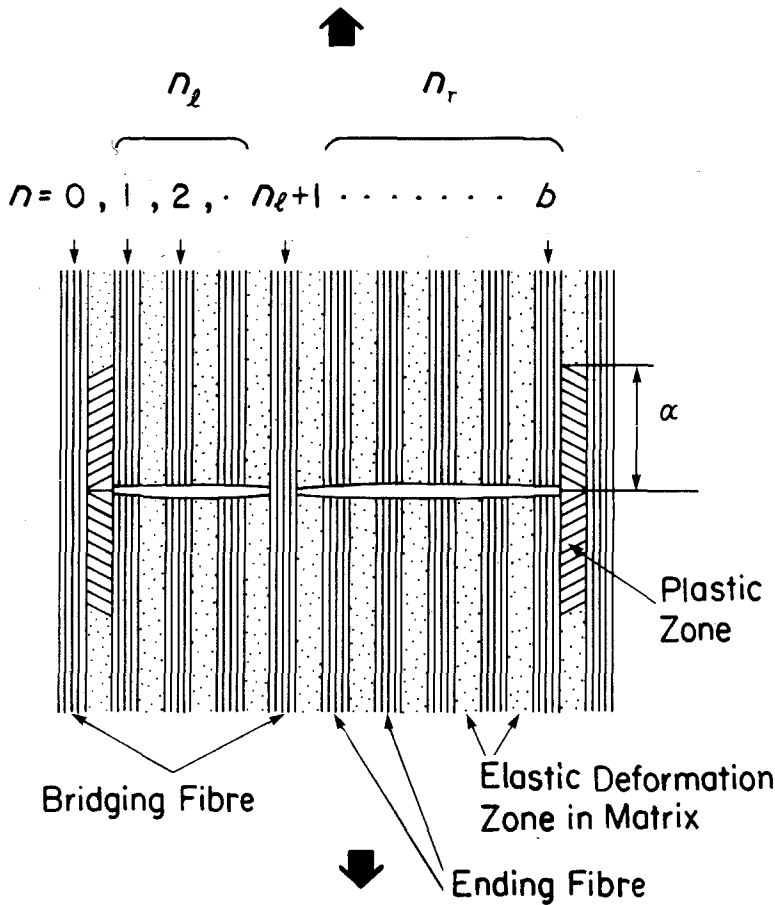
Figure 3 Model of stress concentration calculations for a fibre-end-gap in discontinuous fibre composite with matrix plastic deformation zone at the tip of the gap.

tively. Another simple approximation for the load sharing rule was used in [10–16], where it is assumed that the stress enhancement of a bridging fibre is given only by the first nearest neighbouring fibre-end-gaps on both sides and the magnitude is

$$\bar{K}_1^u = 1 + \frac{n_l + n_r}{2} \qquad (1)$$

where n_l and n_r are numbers of ending fibres in the left and right fibre-end-gaps. Here, the stress in an ending fibre is transferred to the two nearest intact fibres, so that a bridging fibre with $(n_l + n_r)$ adjacent ending fibres receives an additional load of $(n_l + n_r)/2$. This assumption gives an upper value approximation of stress concentration factor. Thus we obtain

$$\bar{K}_1^l \leqslant \bar{K}_2^l \leqslant \bar{K}_3^l \leqslant \ldots \leqslant \bar{K} \leqslant \bar{K}_1^u \qquad (2)$$

Hereafter we consider the first lower value approximation $(\bar{K}_1^l)$ and upper value approxima-

tion $(\bar{K}_1^u)$ for simplicity, denoted as weak and strong local load sharing rule, respectively. In the case of strong local load sharing rule, clearly, if one bridging fibre fails then the whole composite fails. Thus neglecting the load bearing capacity of the matrix, the strength of the composite was given [10] by

$$X_N = \sigma_{\text{fu}} \bigg/ \left(1 + \frac{J_N}{2}\right) \qquad (3)$$

where J_N is the largest number of ending fibres adjacent to a bridging fibre, σ_{fu} is the fibre tensile strength and N is the total number of fibres in the composite.

In the case involving the weak local load sharing rule, the stress of the ending fibres are redistributed more evenly among the bridging fibres on both sides. Using the shear-lag method (see Fig. 3), the stress concentration factor $\bar{K}_1^l$ in the presence of n_l and n_r ending fibres is obtained as [18]

$$\bar{K}_1^l = U_{n_l+1}^b \Bigg/ \det \begin{bmatrix} & & & n_l+1 & & & \\ & & & \downarrow & & & \\ G_{1,1} & G_{1,2} & . & 0 & . & . & G_{1,b} \\ G_{1,2} & G_{2,2} & . & 0 & . & . & G_{2,b} \\ . & & . & 0 & . & . & . \\ 0 & 0 & 0 & 1 & 0 & 0 & 0 \\ . & & . & 0 & . & . & . \\ G_{b,1} & G_{b,2} & . & 0 & . & . & G_{b,b} \end{bmatrix} \leftarrow n_l+1 \qquad (4)$$

where U_n^b is half of the elastic crack opening displacement [21] at the nth fibre in b broken fibres,

$$U_n^b = \frac{\pi[2(b-n)+1]!(2n-1)!}{2^{2b}[(b-1)!(n-1)!]^2} \qquad (5)$$

and

$$b = n_l + n_r + 1, \quad G_{n,m} = 4/[1-4(n-m)^2]\pi$$

Here we assume that the fibre length is sufficiently large so the stress concentration factor can be calculated from a continuous fibre model. However, in the case of weak local load sharing rule, the failure of the $(n_l + 1)$th fibre does not cause the composite failure since $\bar{K}_1^l$ given in Equation 4 is larger than the stress concentration factor K_b in the 0th bridging fibre after the failure of the $(n_l + 1)$th bridging fibre, (Appendix I). Clearly, the failure of the 0th bridging fibre causes the total failure of the composite. Thus neglecting the load bearing capacity of the matrix, the strength of the composite is given by

$$X_N = \sigma_{fu}/K_b^1 \qquad (6)$$

The explicit expression of elastic stress concentration factor K_b^1 due to b broken fibres is first obtained by Hedgepeth [20] in the context of shear lag analysis

$$K_b^1 = \frac{4 \cdot 6 \cdots (2b+2)}{3 \cdot 5 \cdots (2b+1)} \qquad (7)$$

This result has been lately proved rigorously by Hikami and Chou [18].

The explicit expression of K_b^1 for composites with plastically deformed matrices has also been obtained by Hikami and Chou [21]. For the small scale plastic deformation case, the plastic stress concentration factor $\tilde{K}_b^1$ can be expressed in series expansion form in terms of the dimensionless plastic deformation zone length α. The first approxi-

mation gives

$$\tilde{K}_b^1 \simeq K_b^1 \left(1 - \frac{b}{2b+1} \frac{\alpha^2}{2}\right) \qquad (8)$$

where

$$\alpha \simeq \frac{\pi b(b+1)}{2(K_b^1)^2(2b+1)} - \frac{1}{K_b} \left(\frac{T_0}{\sigma_\infty}\right) \qquad (9)$$

Matrix plastic deformation takes place when the applied stress exceeds the critical value $\sigma_{\infty c} \ (= T_0/U_1^b)$ where

$$T_0 = \tau_y(dEh/GA)^{1/2} \qquad (10)$$

The shear strength of the matrix, the shear modulus of the matrix and the stiffness of the fibre are denoted as τ_y, G and E, respectively. The fibre spacing, the fibre cross-sectional area, and the thickness per fibre are also denoted as d, A and h, respectively. For the large scale plastic deformation case, the fibre stress concentration factor at the tip of a fibre-end-gap can be well approximated by

$$\tilde{K}_b^1 \simeq 1 + \frac{2}{\pi} \left(\frac{T_0}{\sigma_\infty}\right) [\ln(b\sigma_\infty/T_0) + \gamma'] \qquad (11)$$

where γ' is the Euler's constant ($\cong 0.577$).

2.2. Probability distribution of maximum fibre-end-gap

The fibre-end-gap is modelled for the case of the two-dimensional array shown in Fig. 1a. The size of the critical zone [8] is denoted by βl. Focusing the attention on a single fibre-end, the probability, P_n, that this fibre-end is in the gap consisting of n fibre-ends is

$$P_n = n\beta^{n-1}(1-\beta)^2 \qquad (12)$$

and

$$\sum_{n=1}^{\infty} P_n = 1. \qquad (13)$$

Equation 12 is an improvement of the corresponding result of Fukuda and Chou [9]. The difference
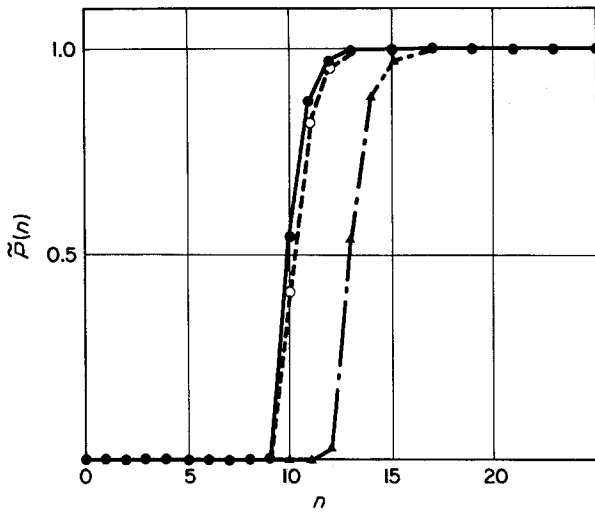
Figure 4 Cumulative probability distribution functions for the maximum fibre-end-gap size. ○: $N = 10^6$, $\beta = 0.2$; ●: $N = 10^6$, $\beta = 0.1$; ▲: $N = 10^8$, $\beta = 0.2$.

in P_n between the present Equation 12 and the result of Fukuda and Chou becomes significant when n and β are large.

The probability that a given fibre-end is not in any one of the gaps with more than n fibre ends is

$$Q_n = 1 - \sum_{i=n+1}^{\infty} P_i. \qquad (14)$$

When the above probability is independent for each fibre, the probability that there is no gap larger than size n is

$$\tilde{P}(n) = (Q_n)^N \qquad (15)$$

where N is the total number of fibres in the composite. However, actually Q_n for a given fibre is not independent of the other fibres. When N is sufficiently larger than the average gap size $\bar{n}$, it is more suitable to express $\tilde{P}(n)$ of Equation 15 as

$$\tilde{P}(n) = (Q_n)^{N/\bar{n}} \qquad (16)$$

where

$$\bar{n} = \sum_{n=1}^{\infty} nP_n. \qquad (17)$$

Using Equations 12 and 14, Equation 16 can be rewritten as

$$\tilde{P}(n) = \{1 - \beta^n [n(1-\beta) + 1]\}^{N\beta'} \qquad (18)$$

and

$$\beta' = \frac{1}{\bar{n}} = \frac{1-\beta}{1+\beta}. \qquad (19)$$

$\tilde{P}(n)$ can be used to determine the strength of discontinuous fibre composites through the relation between gap size n and the corresponding stress concentration. Fig. 4 demonstrates the variation of $\tilde{P}(n)$ with N and β. It can be shown that $\tilde{P}(n)$ behaves like a step function and $\tilde{P}(n)$ changes from

0 to 1 at $n \cong M$ where M is determined from

$$\beta^n [n(1-\beta) + 1]N\beta' = 1. \qquad (20)$$

M obtained from Equation 20 is termed the "most probable maximum gap size". Fig. 5 shows M as a function of β and N. For actual composites, the values of M do not vary tremendously with β and N. When N is sufficiently large, using the formula $1 - x \cong \exp(-x)$, $\tilde{P}(n)$ can be approximated as

$$\tilde{P}(n) \simeq \exp[-N\beta^n n(1-\beta)^2]. \qquad (21)$$

This result agrees with the asymptotic form of $\tilde{P}(n)$ obtained by Smith [10] for large n.
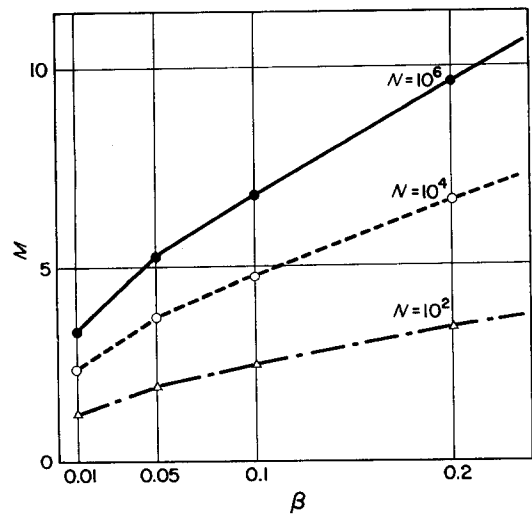
Figure 5 Most probable maximum gap size, M against critical zone parameter, β. N denotes the total number of fibres.

2.3. Modification of rule-of-mixtures

In this section a strength theory is proposed for unidirectional discontinuous fibre composite based upon the probabilisitc approach in Section 2.2. The composite ultimate strength σ_{cu} is defined as the stress level at which fracture of the composite occurs. Consequently, within the first approximation considered in Section 2.1, σ_{cu} is given as

$$\sigma_{cu} = \sigma_\infty V_f + \sigma'_m(1 - V_f) \qquad (22)$$

where σ_∞ represents the applied fibre stress at the moment when the fibre stress at the stress concentration reaches σ_{fu}. Thus σ_∞ satisfies:

$$\sigma_{fu} = \bar{K}_1^l(\sigma_\infty - \eta\sigma_{my}(1 - V_f)/V_f) \quad (23a)$$

for the weak local load sharing rule where $\bar{K}_1^l$ stands for K_b^l (Equation 7) and $\tilde{K}_b^l$ (Equation 8) in elastic and plastic deformations, respectively. Also,

$$\sigma_{fu} = \bar{K}_1^u(\sigma_\infty - \eta\sigma_{my}(1 - V_f)/V_f) \quad (23b)$$

for the strong local load sharing rule. Here, σ'_m is the matrix stress at the ultimate tensile strain of the fibre, σ_{my} is the matrix yield stress, and V_f denotes fibre volume fraction.

$\bar{K}_1^l$ and $\bar{K}_1^u$ represent the stress concentration factors obtained in Section 2.1 (Equations 1, 7, 8, 11). Since the composite fractures from the weakest point, the stress concentration factors $\bar{K}_1^l$ and $\bar{K}_1^u$ for the largest fibre-end-gap in the composite should be used. The average strength of the composite ($= \bar{\sigma}_{cu}$) is then obtained by using the stress concentration factors $\bar{K}_1^l$ and $\bar{K}_1^u$ for the most probable maximum gap size M defined in Section 2.2 (Equation 20). The parameter η in Equations 23a and 23b represents the loading condition of the matrix in the fibre-end-gap. If the matrix is brittle, as in the case of polymer based composite, the crack propagates in the matrix along the fibre-end-gap prior to the failure of the intact bridging fibre. In this case the matrix in the fibre-end-gap will bear no load and η is taken to be 0. However, in metal matrix composites, the matrix in the fibre-end-gap can deform plastically to the yield stress σ_{my}. Then each fibre in the fibre-end-gap sustains the stress $\sigma_{my}(1 - V_f)/V_f$, thus reducing the applied stress σ_∞. We take approximately this effect in Equations 23a and 23b with $\eta = 1$.

3. Strength theory of three-dimensional fibre composites

In the case of three-dimensional fibre array, the problem is more complicated and there is no rigor-
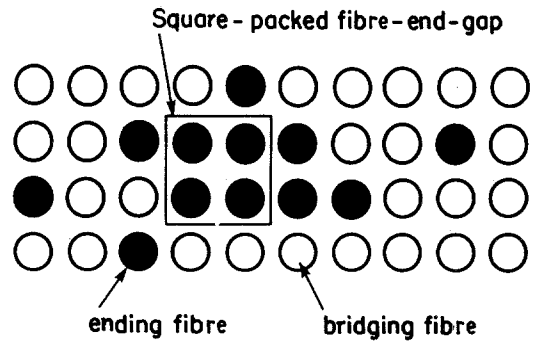
Figure 6 Schematic cross-sectional view of a three-dimensional fibre array. Solid circles indicate ending fibres and open circles for bridging fibres.

ous probabilistic treatment available. The shape of the fibre-end-gap cannot be uniquely defined for a given number of fibre ends and it is fairly involved to obtain the highest stress concentration factor in the intact bridging fibres. Furthermore, the fibre failure process here is more complex than that in the two dimensional case. To circumvent these difficulties, Fukuda and Chou [9] took only compact fibre-end-gaps as the first approximation. Following this approximation, we also consider only special types of fibre-end-gaps which consist of square-arrayed, compact ending fibres. A typical example of such a fibre-end-gap is shown in Fig. 6, where ending fibres are indicated by solid circles and bridging fibres by open circles in the two-dimensional square lattice. We consider the largest square-arrayed group of ending fibres which can be accommodated in a given fibre-end-gap. The size of such a square array may be expressed as $b \times b$ ($b = 1, 2, 3 \ldots$). For example, in Fig. 6 the size of the square array is 2×2. Then the stress concentration factor for the actual fibre-end-gap is approximated by that of the corresponding square array fibre-end-gap. Using this approximation, the probability distribution for the maximum size of square arrayed gap is calculated. First, consider the probability that a given fibre end is not in any one of the gaps with more than n fibre ends. For $0 < \beta \ll 1$, it is approximately given as (Appendix II)

$$Q_n \simeq 1 - (n + 1)^2\beta^{(n+1)^2-1}. \qquad (24)$$

Then the corresponding cumulative probability distribution function $\tilde{P}(n)$ for the maximum fibre-end-gap size becomes

$$\tilde{P}(n) = [1 - (n + 1)^2\beta^{(n+1)^2-1}]^{N/\bar{n}} \quad (25a)$$

where

$$\bar{n} = \sum_{n=1}^{\infty} n[n^2\beta^{n^2-1} - (n+1)^2\beta^{(n+1)^2-1}] \quad (25b)$$

$\tilde{P}(n)$ in three-dimensional fibre composites also behaves like a step function and changes from 0 to 1 at $n \cong M$, where M is the most probable maximum gap size obtained as the solution of

$$N(n+1)^2\beta^{(n+1)^2-1}/\bar{n} = 1. \quad (26)$$

The typical value of M in three-dimensional fibre composites lies between 2 and 4, which is approximately the square root of the typical values of M in two-dimensional fibre composites. The average strength of the composite is then given by Equations 27, 28a and 28b.

$$\tilde{\sigma}_{cu} = \sigma_{\infty}V_f + \sigma'_m(1 - V_f) \quad (27)$$

where

$$\sigma_{fu} = \lambda^l\bar{K}_1^l[\sigma_{\infty} - \eta\sigma_{my}(1 - V_f)/V_f] \quad (28a)$$

for weak local load sharing rule and

$$\sigma_{fu} = \lambda^u\bar{K}_1^u[\sigma_{\infty} - \eta\sigma_{my}(1 - V_f)/V_f] \quad (28b)$$

for strong local load sharing rule.

In Equations 28a and 28b, the three-dimensional stress concentration factors for the most probable maximum gap size M are given as $\lambda^l\bar{K}_1^l$ and $\lambda^u\bar{K}_1^u$, with λ^l and λ^u being the ratio of the three-dimensional concentration factors to the corresponding two-dimensional results.

4. Numerical results and discussions
Numerical calculations are carried out for the strength of discontinuous fibre composite based upon the present theory.

4.1. Composites with elastic matrix
Fig. 7 shows the relation between the fibre volume fraction, V_f and average strength of the composite normalized by the matrix stress at failure, $\tilde{\sigma}_{cu}/\sigma'_m$. In this calculation, we adopted the following properties of a glass fibre reinforced thermoplastic composite [9]. The fibre length l, fibre diameter d_f, fibre critical length l_c, critical zone parameter β are assumed to be 1 mm, 0.01 mm, 0.1 mm and 0.1, respectively. Both the strength ratio σ_{fu}/σ'_m and the Young's modulus ratio, E_f/E_m between the fibre and matrix are taken to be 35.2. The total volume of the composite, V is assumed to be 400 mm³.

In Fig. 7, the line [A] shows the simple rule-of-mixtures for continuous fibres, while the line [B] depicts the rule-of-mixtures modified for discon-
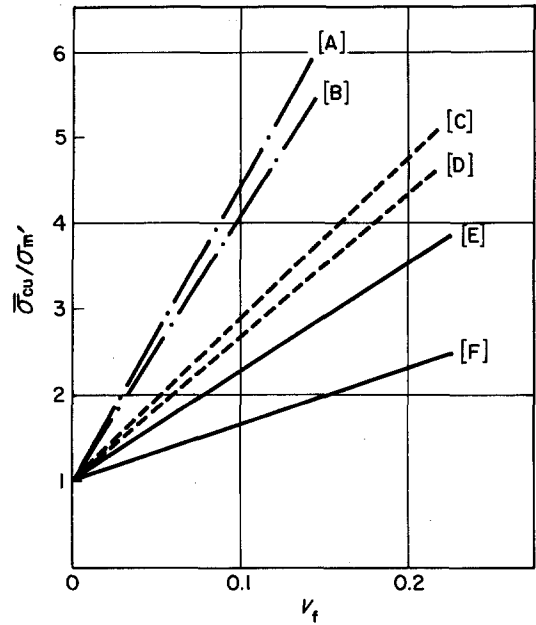
Figure 7 Strength of the composite as a function of V_f. [A]: rule-of-mixtures; [B]: Kelly and Tyson [19]; [C] – [F]: present theory. [C]: 3-dimensional fibre array, weak local load sharing; [D]: 3-dimensional fibre array, strong local load sharing; [E]: 2-dimensional fibre array, weak local load sharing; [F]: 2-dimensional fibre array, strong local load sharing.

tinuous fibres. Both cases do not take the effect of local stress concentrations into consideration. The dotted lines and solid lines depict the present results of three-dimensional fibre array and two-dimensional fibre array, respectively. For each fibre array, upper value approximation and lower value approximation are shown. The lines [C] and [E] represent the lower value approximations of strength based on the weak local load sharing rule while the lines [D] and [F] represent the upper value approximations based on the strong local load sharing rule. The composite strength is expected to lie between these two bounds. The predicted strength of the present theory is far less than the value predicted from the rule-of-mixtures because of local stress concentrations.

The effect of local stress concentration increases as the size of the composite increases, which causes the size effect of composite strength. Fig. 8 indicates the effect of composite size on composite strength for two-dimensional (solid lines) and three-dimensional (dotted lines) fibre arrays. V_f is assumed to be 0.2 and the same material constants as in Fig. 7 are used. For simplicity λ in Equations 28a and 28b is taken to be
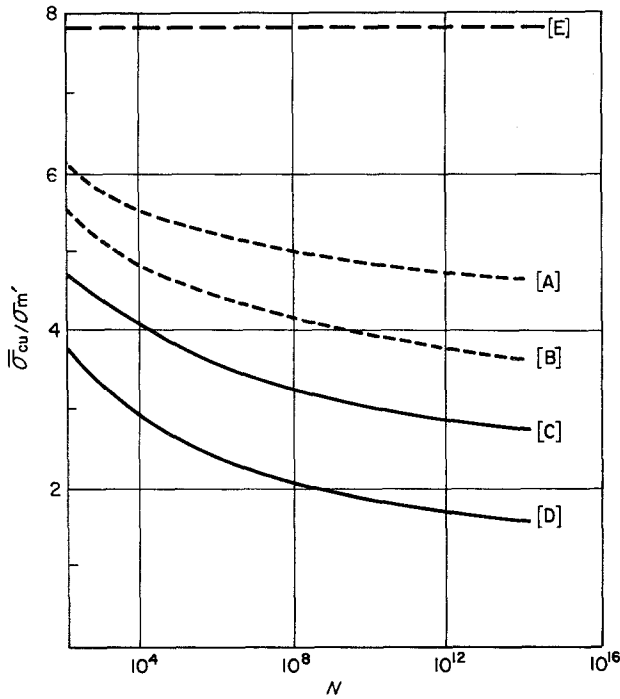
Figure 8 Strength of composite $\bar{\sigma}_{cu}$ normalized by σ'_m against total number of fibres N. Matrix deforms elastically. [A]: 3-dimensional, weak local load sharing; [B]: 3-dimensional, strong local load sharing; [C]: 2-dimensional, weak local load sharing; [D]: 2-dimensional, strong local load sharing; [E]: rule-of-mixtures.

1. The strength of the composite decreases monotonically with increasing N. For sufficiently large value of N, the strength of the composite is estimated by the following upper and lower bounds.

$$\frac{V_f \sigma_{fu}}{1 + \frac{1}{2}\left[\ln N \Big/ \ln \frac{1}{\beta}\right]} + (1 - V_f)\sigma'_m \lesssim \bar{\sigma}_{cu}$$

$$\lesssim \frac{V_f \sigma_{fu}}{\frac{\pi^{1/2}}{2}\left[\ln N \Big/ \ln \frac{1}{\beta}\right]^{1/2}} + (1 - V_f)\sigma'_m \qquad (29a)$$

(two-dimensional fibre array)

$$\frac{V_f \sigma_{fu}/\lambda}{1 + \frac{1}{2}\left\{\left[\ln N \Big/ \ln \frac{1}{\beta}\right]^{1/2} - 1\right\}} + (1 - V_f)\sigma'_m \lesssim \bar{\sigma}_{cu}$$

$$\lesssim \frac{V_f \sigma_{fu}/\lambda}{\frac{\pi^{1/2}}{2}\left\{\left[\ln N \Big/ \ln \frac{1}{\beta}\right]^{1/2} - 1\right\}^{1/2}} + (1 - V_f)\sigma'_m$$

(three-dimensional fibre array)

(29b)

In deriving Equations 29a and 29b, the stress concentration factor is approximated by

$$K_M = \frac{4 \cdot 6 \cdot 8 \cdots (2M + 2)}{3 \cdot 5 \cdot 7 \cdots (2M + 1)} \simeq \left(\frac{\pi^{1/2}}{2}M\right)^{1/2} \qquad (30)$$

The left-hand side of the above inequalities is derived using the strong local load sharing rule while the right-hand side is derived from the weak local load sharing rule. These relations show that the reduction in composite strength due to increase in composite size is quite significant. The reduction is approximately proportional to $(\ln N)^{-P}$, with P being between 0.5 and 1 for two-dimensional composites and between 0.25 and 0.5 for three-dimensional composites.

4.2. Composites with elastic and perfectly plastic matrices

When plastic deformation of the matrix takes place around a fibre-end-gap, it tends to relax the local stress concentration in the intact bridging fibres. Consequently, the composite strength is expected to approach the value predicted by the modified rule-of-mixtures of Kelly and Tyson [19]. In this section we assume the weak local load sharing rule and discuss how the matrix plasticity affects the local stress concentration and reduces the size effect on composite strength. Fig. 9 shows the relation between the total number of fibres, N and normalized strength, $\bar{\sigma}_{cu}/\sigma'_m$ in the presence of large matrix plastic deformation between the ending fibre and bridging fibre at the tip of the fibre-end-gap. Calculations are carried out using Equations 11, 22 and 23a. The strength
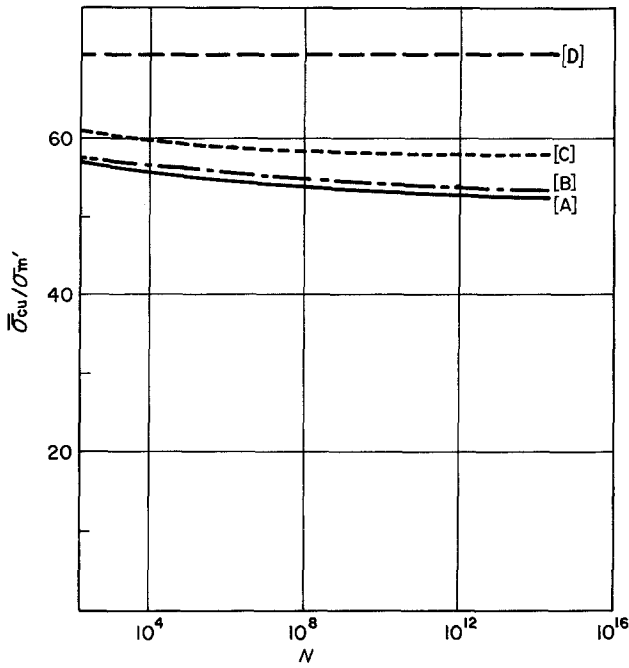
Figure 9 Strength of composite $\bar{\sigma}_{cu}$ normalized by $\bar{\sigma}'_{m}$ against N. Matrix deforms elastically and perfectly plastically. [A]: 2-dimensional, $\eta = 0$; [B]: 2-dimensional, $\eta = 1$; [C]: 3-dimensional, $\eta = 0$; [D]: rule-of-mixtures.

ratio σ_{fu}/σ_{my} is assumed to be 35.2×10, which is ten times larger than the case in Fig. 8. Fibre volume fraction V_f is taken to be 0.2. In this figure the line [A] represents the two-dimensional fibre array with $\eta = 0$ while line [B] corresponds to $\eta = 1$. The line [C] is for three-dimensional fibre array with $\eta = 0$. It can be seen that the composite strength values are not far from those predicted by the rule-of-mixtures (line [D]) and the size effect on the strength is quite weak. Furthermore, it is shown that the load bearing condition of the matrix material in the fibre-end-gap (η) has a rather small effect on the strength when σ_{fu}/σ_{my} is sufficiently large, and thus η is assumed to be zero in the subsequent calculations.

Figs. 10 and 11 show the effect of matrix yield strength on the strength of composites for two-dimensional and three-dimensional fibre arrays. The abscissa represents the dimensionless matrix shear strength Z.

$$Z = (\tau_y/\sigma_{fu})(E_f dh/GA)^{1/2}. \qquad (31)$$

The ordinate is the effective strengthening ratio F [9], which represents the reduction of the reinforcement effect due to the discontinuity and defined as in Equation 32.

$$\bar{\sigma}_{cu} = V_f \sigma_{fu} F + (1 - V_f)\sigma'_m. \qquad (32)$$

We adopt for example, $\beta = 0.1$ and $\eta = 0$, and assume that fibre length, l is sufficiently large compared with l_c. In the following, we consider two limiting cases of matrix behaviour. First, if the
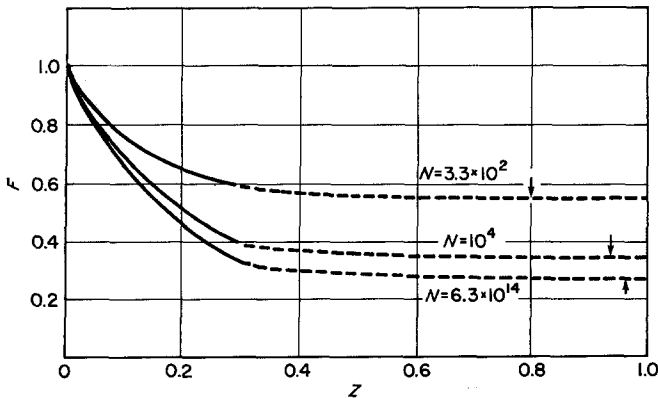
Figure 10 Effective strengthening ratio, F of two-dimensional fibre array against nondimensional matrix yield stress. Z. Arrows indicate the onsets of matrix plastic deformation. N is the total number of fibres.
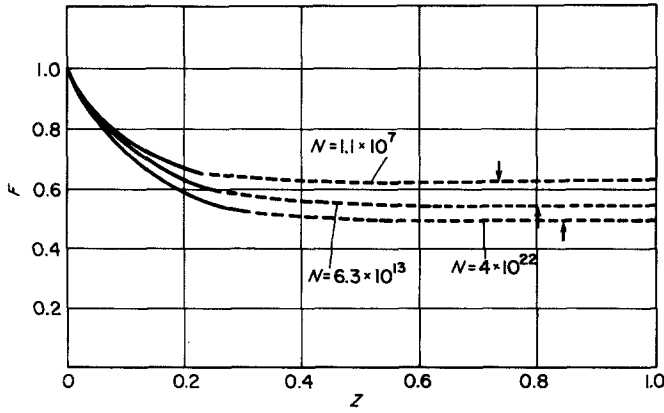
Figure 11 F of three-dimensional fibre array against Z. Arrows indicate the onsets of matrix plastic deformation. N is the total number of fibres.

shear strength of the matrix is large, there is little stress relaxation by plastic deformation at the sites of stress concentrations. Thus F is given as

$$F = \frac{1}{K_M^1} = \frac{(2M+1)!}{2^{2M}M!(M+1)!} \qquad (33)$$

where the most probable maximum gap size M is given by Equation 20 for two-dimensional fibre array and by Equation 26 for three-dimensional fibre array. Second, the matrix shows plastic deformation at the tip of a fibre-end-gap if $Z < Z_0$ where [21]

$$Z_0 = \frac{\pi(2M-1)!(2M+2)!}{2^{4M+1}[(M+1)!(M-1)!]^2}. \qquad (34)$$

Within the small scale plastic deformation condition, $(0 < Z_0 - Z \ll Z_0)$, the effective strengthening ratio F is given by the following equation derived from Equation 8.

$$F = \frac{1}{K_M^1 \left[1 - \dfrac{M}{2M+1} \dfrac{(Z-Z_0)^2}{2} \right]} \qquad (35)$$

$$(\text{for } 0 < Z_0 - Z \ll 1)$$

Third, for the large scale plastic deformation condition $(0 < Z \ll Z_0)$, F is given from Equation 11, as the solution of

$$F + \frac{2}{\pi} Z \left(\ln M \frac{F}{Z} + \gamma' \right) = 1. \qquad (36)$$

It can be shown that F in Equation 36 is asymptotically expressed as

$$F \sim 1 - \frac{2}{\pi} Z \left(\ln \frac{M}{Z} + \gamma' \right) \qquad (37)$$

for small Z. In Figs. 10 and 11, the onset of matrix plastic deformation is expressed by the arrow. The total numbers of fibres, N are also denoted in the figure. For each case of composite size, the effective strengthening ratio F is calculated from Equation 35 for small scale plastic deformation condition and from Equation 36 for large scale plastic deformation condition and the results are indicated by the solid lines. The dotted lines are the results from Equation 36. As expected, the size effect on the strength of composites decreases rapidly as Z approaching zero.

As the matrix plastic deformation grows between the ending fibre and the intact bridging fibre, its extent may exceed the fibre length before the intact bridging fibre fails. This situation arises if the following condition is met

$$Z \leqslant \frac{\sigma_\infty}{\sigma_{fu}} \frac{1}{l} \left(\frac{E_f dA}{Gh} \right)^{1/2} \qquad (38)$$

In this case the high ductility of the matrix annihilates the local stress concentration, when it has little effect on composite strength. Consequently, the modified rules-of-mixtures of Kelly and Tyson [19] essentially gives a reasonable approximation for the strength prediction.

5. Conclusions

The strength of unidirectional discontinuous fibre composites is studied based upon a probabilistic model of fibre configuration. The present theory quantifies the influence of matrix stress transfer properties on composite strength. The main findings are as follows.

1. The analysis adopts the concept of critical zone with ending and bridging fibres first developed by Bader *et al.* and further develops the probabilistic approach of Fukuda and Chou by considering the maximum stress concentration caused by the most probable maximum fibre-end-gap.

2. A limiting case of the present probabilistic model gives good agreement with the analytical results for two-dimensional composites obtained by Smith.

3. For matrices deforming elastically, the local stress concentration around fibre-end-gaps reduce the strength of a composite to a level far less than the value predicted from the rule-of-mixtures. The upper and lower bounds for the effective strengthening ratio F (Equation 32) are obtained. When the size of a composite, N is sufficiently large, F is shown to be proportional to $(\ln N)^{-P}$, with the exponent P being between 0.5 and 1 for two-dimensional composites, and between 0.25 and 0.5 for three-dimensional composites.

4. The strength of composites with plastically deformable matrices is predicted for small scale and large scale plastic deformation conditions. Equation 37 qualitatively shows how the composite strength approaches the modified rule-of-mixtures predicted by Kelly and Tyson.

5. Quantitative comparison of the present theory with experiments is not feasible at the present because of the lack of data from highly controlled measurements.

Acknowledgement

Appendix I: Estimate of Equation 4

Fig. 3 shows the schematic representation for the isolated bridging fibre surrounded by n_l and n_r ending fibres. Here we consider the elastic stress concentration factor $K^*_{n_l, n_r}$ for the isolated bridging fibre is given by

$$K^*_{n_l, n_r} = U^b_{n_l+1} / L^{*b}_{n_l+1, n_l+1} \qquad (A1)$$

where

$$U^b_{n_l+1} = \pi(2n_r + 1)!(2n_l + 1)!/2^{2b}(n_r! n_l!)^2 \qquad (A2)$$

$$L^{*b}_{n_l+1, n_l+1} = \frac{\Delta n_l + 1, n_l + 1}{\det \tilde{L}^b} \qquad (A3)$$

$\tilde{L}^b$ represents the $(b \times b)$ matrix with its components given by $[\tilde{L}]_{i, j} = (4/\pi)[4(i-j)^2 - 1]^{-1}$, $\Delta n_l + 1, n_l + 1$ denotes the $(n_l + 1, n_l + 1)$ component of the adjoint matrix. Using the approxi-

mations of Equations A4 and A5, $K^*_{n_l, n_r}$ can be evaluated as follows.

$$\Delta_{m+1, m+1} \cong \det \tilde{L}^{(n)} \det \tilde{L}^{(m)} \qquad (A4)$$

$$\det \tilde{L}^{(*)} \cong 1 \qquad (A5)$$

$$K^*_{n_l, n_r} \cong U^b_{n_l+1} \qquad (A6)$$

The stress concentration factor for the 0th fibre on the edge of the fibre-end-gap after the breakage of the isolated bridging fibre is given by

$$K^2_b = \frac{4 \cdot 6 \cdot 8 \cdots (2b + 2)}{3 \cdot 5 \cdot 7 \cdots (2b + 1)} \qquad (A7)$$

Since $U^b_{n_l+1} \geqslant U^b_2$ for $b - 2 \geqslant n_l \geqslant 1$, we obtain the following inequality.

$$\frac{K^*_{n_l, n_r}}{K_b} \gtrsim \frac{U^b_2}{K_b} = \frac{3\pi}{4} \frac{(2b - 3)!!}{(2b - 4)!!} \frac{(2b + 1)!!}{(2b + 2)!!} \gtrsim 1. \qquad (A8)$$

Appendix II: Derivation of Equation 24

Since any ending fibre is situated in a fibre-end-gap, clearly $Q_0 = 0$, which is consistent with Equation 24. Then consider the probability that a given ending fibre is in a fibre-end-gap whose size is equal to or greater than two $(= 1 - Q_1)$. Fig. A1 shows the schematic configuration of fibres corresponding to the above event. The given ending fibre is located at $(0, 0)$. This ending fibre would be in one of the following fibre-end-gaps.

Fibre-end-gap No. 1: $(0, 0)$, $(0, 1)$, $(1, 0)$, $(1, 1)$
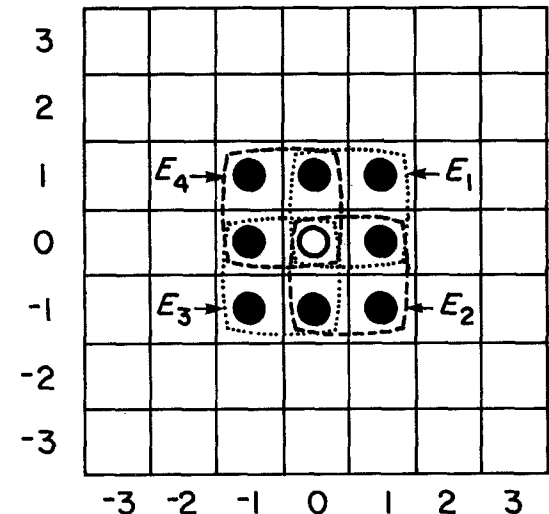
Figure A1 The ending fibre configuration.

No. 2: $(0,0)$, $(0,-1)$,
$(1,0)$, $(1,-1)$

No. 3: $(0,0)$, $(0,-1)$,
$(-1,0)$, $(-1,-1)$

No. 4: $(0,0)$, $(0,1)$,
$(-1,0)$, $(-1,1)$

We define the events corresponding to these fibre-end gaps as E_1, E_2, E_3 and E_4. Then

$$1 - Q_1 = Pr(E_1 \cup E_2 \cup E_3 \cup E_4) = \sum_{i=1}^{4} Pr(E_i)$$

$$- \sum_{i \neq j} Pr(E_i \cap E_j) + \sum_{i \neq j \neq k} Pr(E_i \cap E_j \cap E_k)$$
$$- Pr(E_1 \cap E_2 \cap E_3 \cap E_4)$$
$$= 4\beta^3 - 5\beta^5 - 2\beta^6 + 4\beta^7 - \beta^8 \qquad \text{(B1)}$$

For $0 < \beta \ll 1$, the above equation can be approximated as

$$1 - Q_1 \simeq 4\beta^3. \qquad \text{(B2)}$$

Using the same approximation for $1 - Q_n$ we obtain

$$1 - Q_n \simeq (n+1)^2 \beta^{(n+1)^2 - 1}. \qquad \text{(B3)}$$

References

1. T. W. CHOU and A. KELLY, *Mater. Sci. Eng.* **25** (1976) 35.
2. *Idem, Ann. Rev. Mater. Sci.* **10** (1980) 229.
3. J. R. VINSON and T. W. CHOU, "Composite Materials and Their Use in Structures," (Elsevier-Applied Science, London, 1975).
4. P. W. MANDERS and T. W. CHOU, *Proc. ICCM4* (1982) 1075.
5. H. EDWARD and N. P. EVANS, *Proc. ICCM3* (1980) 1620.
6. H. RICHTER, *Proc. ICCM3* (1980) 387.
7. K. D. KACIR and M. NARKIS, *Polym. Eng. Sci.* **15** (1975) 525.
8. M. G. BADER, T. W. CHOU and J. QUIGLEY, "New Developments and Applications in Composites," edited by D. Wilsdorf (The Metallurgical Society-American Institute of Mining Metallurgy and Petroleum Engineering, New York, 1979) p. 127.
9. H. FUKUDA and T. W. CHOU, *J. Mater. Sci.* **16** (1981) 1088.
10. R. L. SMITH, *Stochastic Process Appl.* submitted.
11. D. G. HARLOW and S. L. PHOENIX, *J. Compos. Mater.* **12** (1978) 195.
12. *Idem, ibid.* **12** (1978) 314.
13. *Idem, Int. J. Fract.* **15** (1979) 321.
14. *Idem, ibid.* **17** (1981) 347.
15. *Idem, ibid.* **17** (1981) 601.
16. R. L. SMITH, *Proc. R. Soc. Lond.* **A372** (1980) 539.
17. C. W. ANDERSON, *J. Appl. Probab.* **7** (1970) 99.
18. F. HIKAMI and T. W. CHOU, submitted for publication.
19. A. KELLY and W. R. TYSON, *J. Mech. Phys. Solids* **13** (1965) 329.
20. J. M. HEDGEPETH, "Stress Concentration in Filamentary Structure," NASA TN D-882 (1961).
21. F. HIKAMI and T. W. CHOU, submitted for publication.